Supporting Information for

The Proapoptotic G41S Mutation to Human Cytochrome *c* Alters the Heme Electronic Structure and Increases the Electron Self-Exchange Rate

Matthew D. Liptak, Robert D. Fagerlund, Elizabeth C. Ledgerwood, Sigurd M. Wilbanks, Kara L. Bren

Contents

Supplementary Methods

Protein Expression and Purification. The G41S mutation was introduced into the human (*Hs*) cytochrome (cyt) *c* expression vector pBTR(Human Cc) as described previously.[1] WT and G41S *Hs* cyt *c* were expressed in *Escherichia coli* strain BL21(DE3). 2 mL cultures in Terrific Broth (TB) were shaken for 3-4 h at 37 ºC and used to inoculate 500 mL of TB in a 2 L flask. The culture was shaken at 37 ºC for 24 h and the cells were harvested by centrifugation. The cell pellet was resuspended in 20 mL ice-cold phosphate buffered saline (PBS), sonicated for 5 min (Branson, 40 % duty cycle, power 4), and centrifuged. Ammonium sulfate was gradually added to the supernatant to a final concentration of 35 % (w/v). After centrifugation, the supernatant was dialyzed overnight at 4 ºC against 2 × 4 L low salt buffer [50 mM sodium phosphate (NaP_i), pH 7.3]. The dialysate was filtered and loaded on a FPLC HiTrap SP Sepharose column (GE Scientific) equilibrated in low salt buffer. Cyt *c* was eluted using a linear gradient from 100 % low salt buffer to 100 % high salt buffer [low salt buffer + 1 M sodium chloride (NaCl)]. The eluted cyt *c* was concentrated and loaded on a FPLC Sephadex S75 column (GE Scientific) equilibrated in 50 mM NaP_i, pH 7.3, 50 mM NaCl. Fractions were analyzed by determining the ratio of A_{410} to A_{280} and fractions with a ratio > 4.0 were considered pure. The concentration was determined from A_{410} using an extinction coefficient of 106.1 $mM^{-1}cm^{-1}$.[2] Fractions were stored at -80 ºC. Intact mass measurement of purified cyt *c* variants was performed by high-resolution mass spectrometry using an Orbitrap XL mass analyzer operated at a resolution (FWHM) of 60,000-100,000. Prior to nuclear magnetic resonance (NMR) sample preparation the proteins were dialyzed against mQ water and lyophilized.

Crystallization Structure Determination. Crystals were grown by the hanging-drop vapor diffusion method in a modification of the procedure of Sanishvili et. al.[3] To prepare hanging drops, protein at 12.5 mg/mL in 50 mM NaP_i, 50 mM NaCl, pH 7.0 was dialyzed against 22.5 % (w/v) polyethylene glycol 1000 (PEG-1000), 50 mM monobasic potassium phosphate (KP_i), 5 mM dithiothreitol (DTT) pH 7.0 with NaOH. Hanging drops of 2 μL of this solution (no reservoir buffer)

were allowed to equilibrate above 30 % (w/v) PEG-1000, 45 mM KP_i, 5 mM DTT pH 7.0. Crystals grew as plates of more than 0.2 mm in extent at 16 °C in one to two days. Crystals were transferred to a 10 % (v/v) solution of glycerol in the well solution and mounted in a loop at -180 °C. The most promising crystal diffracted to ~1.7 Å with mosaicity of ~1.3°. Data were collected on a Rigaku MSC 007HF rotation copper anode running at 40 kV and 30 mA with Osmic VariMax optics collimated to 0.3 mm. CrystalClear was used to collect 180° of data in 0.5° oscillations with exposure time of 40 minutes per degree on a Raxis IV++ image plate set at 100 mm from the crystal with $2\theta = 0°$.

Data were indexed in space group C2, with unit cell dimensions of 184.63, 62.69, and 35.47 Å and $\beta = 89.78$, integrated and scaled using d*trek.[4] The data were subsequently converted to mtz format and data intensities converted to structure factors using the program Dtrek2mtz from the CCP4 suite;[5] 5 % of the reflections were reserved for the calculation of the R_{free} statistics. Data collection and reduction statistics are given in Table S1.

Programs of the CCP4 suite were used.[5] Phases were solved by molecular replacement using our earlier, 2.7 Å, structure of G41S *Hs* cyt *c*[1] as a search model in Phaser.[6] Four monomers were placed in the asymmetric unit and phases improved by solvent flattening with tight non-crystallographic symmetry (NCS) restraints (residues 1-104 of each chain) in DM,[7] followed by ARP/wARP.[8] Automated model refinement was performed in Refmac 5.5 using phases from ARP/wARP,[9] fourteen TLS groups defined in TLSMD and relaxed NCS restraints.[10] Models were inspected in COOT and manual adjustment was performed to match chemical expectations and electron density maps.[11] A final round of refinement in Refmac 5.5 used diffraction data to 1.9 Å, but neither NCS nor prior phase information (Table S2).

Crystallographic Model. All chains of the model are similar, with chains A and B particularly so, as are chains C and D (RMSD 0.069 Å in both cases) while other pairs show RMSDs of 0.15 to 0.16 Å. Crystal packing also shows similarity within those pairs, with chain A making contacts with chains B and C (as well as symmetry mates of itself) which are analogous to those made by chain B with chains

A and D and its own symmetry mates, respectively. Similarly, chain C makes contacts analogous to those made by chain D. It appears that a small rearrangement of the polypeptides could reduce the observed packing to a higher symmetry space group with two polypeptide chains in the asymmetric unit. Attempts to index our data with higher symmetry were not successful.

All 104 residues of each chain are resolved in the final model and possess acceptable geometry. The Ramachandran plots showed 411 residues in allowed positions, 5 in generously allowed regions, and 4 (Asn27 of each chain) in a disallowed region. The electron density supports the model at Asn27 and superposition with cyts *c* from other species shows no significant differences.

There is a pseudo-symmetrical interaction between the omega loops of chains A and B, comprising four direct contacts per pair of molecules: apparent hydrogen bonds linking the hydroxyl of Ser47 with carbonyl of Gly45 and the carboxylate of Gln42 with ε amino group of Lys53. These contacts are not present in chains C and D. In chains A and B, the position of Pro44 is displaced by 1.4 Å relative to that seen in chains C and D, likely as a result of these intermolecular interactions. However, the nearby environments surrounding heme propionate 7 (Figure 1) are indistinguishable in all four chains of our crystallographic model. Nonetheless, we concentrated our analysis of the conformation observed for the loops surrounding the position of the G41S mutation on chains C and D, to avoid any artifact resulting from the crystal environment. Arg38 appears to occupy two positions; the major position has been modeled and is indistinguishable in the four chains. The alternate position in each chain is closer to propionate 7, similar to cyts *c* from yeast and horse.

NMR Resonance Assignments. Lyophilized WT and G41S *Hs* cyt *c* were dissolved to final concentrations of 1-3 mM in 100 mM NaP_i buffer (pH 7.0) prepared using 99.9 % deuterium oxide (D_2O, Cambridge Isotope Laboratories). Note, the pH meter readings reported in this work have not been adjusted to account for the presence of deuterium. Oxidized (Fe^{3+}) NMR samples were prepared by adding potassium ferricyanide to a final concentration of 15 mM. Reduced (Fe^{2+}) NMR samples were prepared from Ar(g)-purged protein solutions; an Ar(g) purged dithionite solution in 100 mM NaP_i

buffer (100 % D_2O, pH 7.0) was added under Ar(g) to a final concentration of 15 mM. The reduced NMR samples were loaded into low pressure/vacuum (LPV) NMR sample tubes (Wilmad-Labglass) under a N_2(g) atmosphere. Following NMR data collection, the pH of the oxidized WT, oxidized G41S, reduced WT and reduced G41S *Hs* cyt *c* NMR samples was 7.0, 7.0, 6.8 and 6.6, respectively.

All NMR experiments were performed at 25 °C on a Varian Inova 500-MHz spectrometer equipped with a triple-resonance probe. ^{1}H-^{1}H double quantum filtered correlated spectroscopy (DQF-COSY) and ^{1}H-^{1}H nuclear Overhauser enhancement spectroscopy (NOESY) experiments with oxidized cyt *c* NMR samples both utilized recycle times of 600 ms, with a mixing time of 60 ms for the NOESY experiments. ^{1}H-^{13}C heteronuclear multiple quantum coherence (HMQC) experiments with these oxidized cyt *c* samples used 300-ms recycle times and 2.5-ms refocusing times (J_{CH} = 200 Hz). For reduced cyt *c* NMR samples, ^{1}H-^{1}H total correlation spectroscopy (TOCSY) and NOESY experiments employed recycle times of 1.2 s with a mixing time of 100 ms (NOESY) or a spin-lock time of 45 ms (TOCSY). The HMQC experiments on reduced cyt *c* samples utilized recycle times and refocusing times of 600 ms and 3.5 ms (J_{CH} = 140 Hz), respectively. ^{1}H NMR spectra (3-s recycle time) were collected before and after every two-dimensional NMR experiment to verify sample integrity.

All two-dimensional NMR data was processed in NMRPipe with a pure cosine-squared window function applied to both dimensions.[12] The raw data was zero-filled, and forward linear-prediction was used to double the number of points in the indirect dimension, prior to applying a Fourier transform to obtain 4096 × 4096 (DQF-COSY, TOCSY, and NOESY) or 2048 × 2048 (HMQC) square data matrices. Finally, a polynomial baseline correction was applied to the two-dimensional NMR data. Complete NMR processing scripts are available (Tables S3-S4).

All NMR resonance assignments were made in Sparky,[13] aided by existing assignments for oxidized horse cyt *c*,[14,15] and reduced *Hs* cyt *c*.[16] The DQF-COSY and TOCSY spectra were used to assign propionate and thioether side-chain ^{1}H spin systems. Next, specific ^{1}H resonance assignments were made based upon the through-space connectivities identified in the NOESY spectra. Finally, the

HMQC data was utilized to make specific ^{13}C resonance assignments based upon the one-bond ^{1}H–^{13}C cross-peaks. The ^{1}H and ^{13}C HFSs were determined by subtracting the chemical shifts of reduced cyt *c* from those of oxidized cyt *c*. The ^{1}H and ^{13}C resonances of the propionate side-chains could not be assigned using a natural abundance sample of reduced cyt *c*. Instead, the HFSs of these resonances were determined by subtracting the published chemical shifts of a ^{13}C,^{15}N-enriched sample of reduced WT *Hs* cyt *c* (BMRB ID 5406)[16] from the chemical shift of oxidized *Hs* cyt *c*. Complete ^{1}H and ^{13}C resonance assignments and HFSs are tabulated in Table S5.

Saturation Transfer NMR. 0.5-1.5 mM WT and G41S *Hs* cyt *c* samples were exchanged into 50 mM sodium acetate buffer (pH 5.5) using a PD-10 desalting column (Amersham Biosciences) and reduced with a five-fold excess of ascorbic acid (Sigma). Following reduction, *Hs* cyt *c* samples were exchanged into 100 mM NaP_i buffer (pH 7.0) on a PD-10 column and the concentration was reduced to 500 μL with an Amicon stirred ultrafiltration cell (Millipore) under a N_2(g) atmosphere. Each sample was flash-frozen in liquid N_2, lyophilized, reconstituted with 500 μL of Ar(g)-purged D_2O, and loaded into a LPV NMR tube under a N_2(g) atmosphere.

A series of time-dependent saturation transfer ^{1}H NMR experiments were performed where the Met80 ε-$C^{1}H_3$ resonance of reduced (Fe^{2+}) *Hs* cyt *c* was monitored following saturation of the Met80 ε-$C^{1}H_3$ resonance of oxidized (Fe^{3+}) *Hs* cyt *c*.[17] The saturation time was varied in: 10-ms increments between 0 and 100 ms, 25-ms increments between 100 and 500 ms, 100-ms increments between 500 and 1000 ms, and 1-s increments between 1 and 4 s. The recycle time and acquisition time were held constant at 5 and 1 s, respectively, by adjusting the length of the pre-saturation delay. A ^{1}H NMR spectrum was collected before and after each series of saturation transfer experiments to ensure that the ratio of oxidized to reduced *Hs* cyt *c* remained constant. Following NMR data collection, the total *Hs* cyt *c* concentrations were determined spectrophotometrically on a Shimadzu UV-2401 PC spectrophotometer at an isosbestic point for oxidized and reduced WT *Hs* cyt *c* ($\varepsilon_{410\,nm}$ = 106.1 $mM^{-1}cm^{-}$

[1]).[2] The concentration of oxidized (Fe^{3+}) *Hs* cyt *c* was determined for each sample based upon the total protein concentration and the ratio of oxidized to reduced *Hs* cyt *c*.

The integrated intensity of the reduced (Fe^{2+}) *Hs* cyt *c* Met80 ε-C^1H_3 resonance was plotted versus saturation time and fit to the following equation using a linear least-squares analysis:[17]

$$M(t) = \frac{M_0}{1 + k_{obs}T_1}\left\{ + k_{obs}T_1 e^{-(k_{obs}+1/T_1)t} \right\}$$

where $M(t)$ is the magnetization of the reduced (Fe^{2+}) *Hs* cyt *c* Met80 ε-C^1H_3 resonance at time t, M_0 is the magnetization at $t = 0$, k_{obs} is the first-order rate constant assuming complete saturation of the oxidized (Fe^{3+}) *Hs* cyt *c* Met80 ε-C^1H_3 resonance, and T_1 is the spin-lattice relaxation time of the reduced Met80 ε-C^1H_3 resonance in the presence of oxidized (Fe^{3+}) *Hs* cyt *c*. The second-order rate constants reported in Figure 3 were determined by dividing k_{obs} by the concentration of oxidized (Fe^{3+}) *Hs* cyt *c*.

Density Functional Theory Calculations. The initial structural model was derived from the X-ray crystal structure of horse cyt *c* (PDB ID 1HRC).[18] All atoms were removed with the exceptions of: Cys14, Cys17, His18, Met80, and the heme *c* cofactor. The protein backbone atoms and β-carbons were removed from all protein residues. Finally, hydrogen atoms were added in ArgusLab to generate an initial structural model with an overall charge of +1.[19] The initial structural model was refined by a restricted geometry optimization of the $S = ½$ ground state with the Gaussian09 software package on the 120 node IBM BladeCenter at the Center for Research Computing of the University of Rochester.[20] During the restricted geometry optimization, the heme(γ-meso)-Fe-His(Nε2)-His(Cε1) and heme(β-meso)-Fe-Met(Sδ)-Met(Cγ) dihedral angles were held at their crystallographic values of 0.7 and 9.5°, respectively. The Gaussian09 calculations used the PBEPBE density functional with the TZVP basis set, density fitting of the Coulomb term, and the CPCM implicit solvent model (ε = 4.00).

Following the restrained geometry optimization, single-point DFT calculations, with and without the ionizable proton of propionate 7, were performed using ORCA 2.6.35 on the IBM BladeCenter at

the University of Rochester.[21] All ORCA calculations used a density functional composed of the Perdew-Wang 91 local density and the Perdew-Burke-Ernzerhof (PBE) generalized gradient functional.[22,23] The resolution of the identity (RI) approximation was used to speed up the calculation of the Coulomb term.[24] These single-point DFT calculations utilized the TZVP basis set with the TZV/J auxiliary basis set.[25,26] The charge screening environment of the protein interior was modeled by using the conductor-like screening model (COSMO) with a dielectric constant of 4.00.[27] The resultant lowest-unoccupied spin-down molecular orbitals and unpaired spin densities were visualized as isosurface plots in gOpenMol with isodensity values of 0.025 and 0.0005 au, respectively (Figures S1-S2).[28]

The electronic **g** and heme methyl ^{13}C **A** tensors were also calculated for both geometric models using coupled-perturbed self-consistent field (CP-SCF) theory with ORCA 2.6.35 on the University of Rochester Center for Research Computing cluster.[21,29] The CP-SCF calculations used the same density functional, RI approximation, and COSMO implicit solvent model as the single-point DFT calculations. For a more flexible treatment of the core orbitals, the **g** and **A** tensor calculations utilized the IGLO-III basis set,[30] with the triply-polarized, "core-properties" basis set on Fe,[31] and the TZV/J auxiliary basis set.[26] All CP-SCF calculations used the IGLO gauge origin and a complete mean-field treatment of spin-orbit coupling.[32] The **A** tensor calculations included the Fermi contact, spin-dipole, and spin-orbit coupling contributions to the hyperfine tensor. Following calculation of the **g** and **A** tensors, the heme methyl ^{13}C HFSs were computed as described previously,[33] based on the method of Moon and Patchkovskii.[34]

Supplementary References.

(1) Morison, I. M.; Cramer Bordé, E. M.; Cheesman, E. J.; Cheong, P. L.; Holyoake, A. J.; Fichelson, S.; Weeks, R. J.; Lo, A.; Davies, S. M. K.; Wilbanks, S. M.; Fagerlund, R. D.; Ludgate, M. W.; Tatley, F.; Coker, M. S. A.; Bockett, N. A.; Hughes, G.; Pippig, D. A.; Smith, M. P.; Capron, C.; Ledgerwood, E. C. *Nature Genet.* **2008**, *40*, 387-389.

(2) Olteanu, A.; Patel, C. N.; Dedmon, M. M.; Kennedy, S.; Linhoff, M. W.; Minder, C. M.; Potts, P. R.; Deshmukh, M.; Pielak, G. J. *Biochem. Biophys. Res. Commun.* **2003**, *312*, 733-740.

(3) Sanishvili, R. G.; Margoliash, E.; Westbrook, M. L.; Westbrook, E. M.; Volz, K. W. *Acta Crystallogr., Sect. D: Biol. Crystallogr.* **1994**, *50*, 687-694.

(4) Pflugrath, J. W. *Acta Crystallogr., Sect. D: Biol. Crystallogr.* **1999**, *55*, 1718-1725.

(5) Bailey, S. *Acta Crystallogr., Sect. D: Biol. Crystallogr.* **1994**, *50*, 760-763.

(6) McCoy, A. J.; Grosse-Kunstleve, R. W.; Adams, P. D.; Winn, M. D.; Storoni, L. C.; Read, R. J. *J. Appl. Crystallogr.* **2007**, *40*, 658-674.

(7) Cowtan, K. *Joint CCP4 and ESF-EACBM Newsletter on Protein Crytallography* **1994**, *31*, 34-38.

(8) Langer, G.; Cohen, S. X.; Lamzin, V. S.; Perrakis, A. *Nat. Protoc.* **2008**, *3*, 1171-1179.

(9) Murshudov, G. N.; Vagin, A. A.; Dodson, E. J. *Acta Crystallogr., Sect. D: Biol. Crystallogr.* **1997**, *53*, 240-255.

(10) Painter, J.; Merritt, E. A. *Acta Crystallogr., Sect. D: Biol. Crystallogr.* **2006**, *62*, 439-450.

(11) Emsley, P.; Cowtan, K. *Acta Crystallogr., Sect. D: Biol. Crystallogr.* **2004**, *60*, 2126-2132.

(12) Delaglio, F.; Grzesiek, S.; Vuister, G. W.; Zhu, G.; Pfeifer, J.; Bax, A. *J. Biomol. NMR* **1995**, *6*, 277-293.

(13) Goddard, T. D.; Kneller, D. G. *Sparky 3*, University of California, San Francisco, CA.

(14) Turner, D. L. *Eur. J. Biochem.* **1993**, *211*, 563-568.

(15) Turner, D. L. *Eur. J. Biochem.* **1995**, *227*, 829-837.

(16) Jeng, W.-Y.; Chen, C.-Y.; Chang, H.-C.; Chuang, W.-J. *J. Bioenerg. Biomembr.* **2002**, *34*, 423-431.

(17) Katki, H.; Weiss, G. H.; Kiefer, J. E.; Taitelbaum, H.; Spencer, R. G. S. *NMR Biomed.* **1996**, *9*, 135-139.

(18) Bushnell, G. W.; Louie, G. V.; Brayer, G. D. *J. Mol. Biol.* **1990**, *214*, 585-595.

(19) Thompson, M. A. *ArgusLab 4.0.1*, Planaria Software LLC, Seattle, WA, http://www.arguslab.com.

(20) Frisch, M. J.; Trucks, G. W.; Schlegel, H. B.; Scuseria, G. E.; Robb, M. A.; Cheeseman, J. R.; Scalmani, G.; Barone, V.; Mennucci, B.; Petersson, G. A.; Nakatsuji, H.; Caricato, M.; Li, X.; Hratchian, H. P.; Izmaylov, A. F.; Bloino, J.; Zheng, G.; Sonnenberg, J. L.; Hada, M.; Ehara, M.; Toyota, K.; Fukuda, R.; Hasegawa, J.; Ishida, M.; Nakajima, T.; Honda, Y.; Kitao, O.; Nakai, H.; Vreven, T.; Montgomery Jr., J. A.; Peralta, J. E.; Ogliaro, F.; Bearpark, M.; Heyd, J. J.; Brothers, E.; Kudin, K. N.; Staroverov, V. N.; Kobayashi, R.; Normand, J.; Raghavachari, K.; Rendell, A.; Burant, J. C.; Iyengar, S. S.; Tomasi, J.; Cossi, M.; Rega, N.; Millam, J. M.; Klene, M.; Knox, J. E.; Cross, J. B.; Bakken, V.; Adamo, C.; Jaramillo, J.; Gomperts, R.; Stratmann, R. E.; Yazyez, O.; Austin, A. J.; Cammi, R.; Pomelli, C.; Ochterski, J. W.; Martin, R. L.; Morokuma, K.; Zakrzewski, V. G.; Voth, G. A.; Salvador, P.; Dannenberg, J. J.; Dapprich, S.; Daniels, A. D.; Farkas, O.; Foresman, J. B.; Ortiz, J. V.; Cioslowski, J.; Fox, D. J. *Gaussian 09, Revision A.02* Wallingford, CT, 2009.

(21) Neese, F. *ORCA 2.6.35*, Universität Bonn, Bonn, Germany, 2008.

(22) Perdew, J. P.; Wang, Y. *Phys. Rev. B* **1992**, *45*, 13244-13249.

(23) Perdew, J. P.; Burke, K.; Ernzerhof, M. *Phys. Rev. Lett.* **1996**, *77*, 3865-3868.

(24) Neese, F. *J. Comput. Chem.* **2003**, *24*, 1740-1747.

(25) Schäfer, A.; Horn, H.; Ahlrichs, R. *J. Chem. Phys.* **1992**, *97*, 2571-2577.

(26) Eichkorn, K.; Weigend, F.; Treutler, O.; Ahlrichs, R. *Theor. Chem. Acc.* **1997**, *97*, 119-124.

(27) Sinnecker, S.; Rajendran, A.; Klamt, A.; Diedenhofen, M.; Neese, F. *J. Phys. Chem. A* **2006**, *110*, 2235-2245.

(28) Laaksonen, L. *gOpenMol 2.32*, Center for Scientific Computing, Espoo, Finland, 2002.

(29) Neese, F. *J. Chem. Phys.* **2001**, *115*, 11080-11096.

(30) Kutzelnigg, W.; Fleischer, U.; Schindler, M. *The IGLO-Method: Ab Initio Calculation and Interpretation of NMR Chemical Shifts and Magnetic Susceptibilities*; Springer-Verlag: Heidelberg, Germany, 1990; Vol. 23.

(31) Neese, F. *Inorg. Chim. Acta* **2002**, *337*, 181-192.

(32) Neese, F. *J. Chem. Phys.* **2005**, *122*, 034107.

(33) Liptak, M. D.; Wen, X.; Bren, K. L. *J. Am. Chem. Soc.* **2010**, *132*, 9753-9763.

(34) Moon, S.; Patchkovskii, S. In *Calculation of NMR and EPR Parameters. Theory and Applications.*; Kaupp, M., Bühl, M., Malkin, V. G., Eds.; Wiley: Weinheim, Germany, 2004.

Table S1. Data Collection and Reduction Statistics

Resolution range (highest shell)	19.88 – 1.90 Å (1.97 – 1.90 Å)
Observed reflections	96928 (9196)
Unique reflections	30928 (3172)
Completeness	96.2 % (93.6%)
I/σ	6.7 (2.9)
R_{merge}[1]	0.098 (0.240)

[1] $R_{merge} = \Sigma|I_{obs}-I_{ave}|/\Sigma I_{ave}$

Table S2. Refinement Statistics

Resolution range (highest shell)	19.79 – 1.90 Å (1.949 - 1.90Å)
Reflections used	29167 (2185)
R_{cryst}[1]	0.17 (0.25)
R_{free}[2]	0.25 (0.35)
Protein and heme atoms in model	3440
Water molecules in model	381
Deviation from ideal bond lengths	0.023 Å
Deviation from ideal bond angles	1.86°
Average B factor	22 ± 9 ± $Å^2$

[1] $R_{cryst} = \Sigma|F_{obs}-F_{calc}|/\Sigma F_{obs}$ computed over a working set composed of 95% of data.
[2] $R_{free} = \Sigma|F_{obs}-F_{calc}|/\Sigma F_{obs}$ computed over a test set composed of 5% of data.

Table S3. ^{1}H-^{1}H COSY, 1H-1H TOCSY, and ^{1}H-^{1}H NOESY Processing Script

```
nmrPipe -in ./test.fid                                          \
| nmrPipe  -fn SP -off 0.5 -end 1.0 -pow 2  -c 1.0              \
| nmrPipe  -fn ZF -size 4096                                    \
| nmrPipe  -fn FT -verb                                         \
| nmrPipe  -fn PS -p0 *.* -p1 *.* -di                           \
| nmrPipe  -fn TP                                               \
| nmrPipe  -fn SP -off 0.5 -end 1.0 -pow 2   -c 0.5            \
| nmrPipe  -fn ZF -size 2048                                    \
| nmrPipe  -fn LP                                               \
| nmrPipe  -fn FT -verb                                         \
| nmrPipe  -fn PS -p0 0.0 -p1 0.0 -di                           \
| nmrPipe  -fn TP                                               \
| nmrPipe  -fn POLY -auto                                       \
      -out ./noesy.dat         -ov
```

* = Optimized for each NMR spectrum

Table S4. ^{1}H-^{13}C HMQC Processing Script

```
nmrPipe -in ./test.fid                                          \
| nmrPipe  -fn POLY -time                                       \
| nmrPipe  -fn SP -off 0.5 -end 1.0 -pow 2  -c 1.0              \
| nmrPipe  -fn ZF -size 2048                                    \
| nmrPipe  -fn FT -verb                                         \
| nmrPipe  -fn PS -p0 *.* -p1 *.* -di                           \
| nmrPipe  -fn TP                                               \
| nmrPipe  -fn SP -off 0.5 -end 1.0 -pow 2   -c 0.5            \
| nmrPipe  -fn ZF -size 1024                                    \
| nmrPipe  -fn LP                                               \
| nmrPipe  -fn FT -verb                                         \
| nmrPipe  -fn PS -p0 0.0 -p1 0.0 -di                           \
| nmrPipe  -fn TP                                               \
| nmrPipe  -fn POLY -auto                                       \
      -out ./hmqc.dat         -ov
```

* = Optimized for each NMR spectrum

Table S5. WT and G41S *Hs* cyt *c* ^{1}H and ^{13}C Resonance Assignments and HFSs

Resonance	WT(Fe^{3+})[a]	G41S(Fe^{3+})[a]	WT(Fe^{2+})[a]	G41S(Fe^{2+})[a]	WT HFS[b]	G41S HFS[b]
CAA	-33.3	-33.2	24.6[c]	24.6[c]	-57.9	-57.8
CBA	135.9	134.5	44.8[c]	44.8[c]	91.1	89.7
CMA	-69.0	-69.0	13.2	13.2	-82.2	-82.2
CMB	-16.9	-16.8	15.4	15.4	-32.3	-32.2
CAB	8.8	9.2	36.1	36.1	-27.3	-26.9
CBB	40.5	39.8	26.4	26.5	14.1	13.3
CMC	-54.2	-55.4	15.2	15.3	-69.4	-70.7
CAC	-36.1	-37.1	39.8	39.9	-75.9	-77.0
CBC	84.4	86.6	22.5	22.5	61.9	64.1
CMD	-23.4	-22.3	15.4	15.4	-38.8	-37.7
CAD	-0.5	0.8	24.6[c]	24.6[c]	-25.1	-23.8
CBD	71.8	70.5	44.1[c]	44.1[c]	27.7	26.4
CHA			98.3	98.1		
CHB			98.4	98.5		
CHC			99.6	99.6		
CHD			99.7	99.8		
HHA	7.85	7.48	9.65	9.63	-1.80	-2.15
HAA1	19.93	18.33	4.19[c]	4.19[c]	15.75	14.15
HAA2	10.51	11.28	3.70[c]	3.70[c]	6.82	7.59
HBA1	1.67	1.54	3.24[c]	3.24[c]	-1.57	-1.70
HBA2	-0.27	-0.33	2.70[c]	2.70[c]	-2.97	-3.03
HMA	35.30	35.66	2.19	2.17	33.11	33.50
HHB	2.61	2.43	9.06	9.05	-6.45	-6.62
HMB	7.19	6.91	3.52	3.52	3.67	3.39
HAB	-1.07	-1.13	5.27	5.27	-6.34	-6.40
HBB	-2.34	-2.34	1.52	1.52	-3.86	-3.86
HHC	1.77	1.92	9.36	9.34	-7.59	-7.42
HMC	32.29	32.98	3.88	3.87	28.41	29.11
HAC	2.12	2.10	6.41	6.40	-4.29	-4.30
HBC	2.94	2.98	2.60	2.60	0.34	0.38
HHD	-0.60	-0.25	9.67	9.66	-10.27	-9.91
HMD	10.16	9.66	3.52	3.52	6.64	6.14
HAD1	2.31	3.26	4.44[c]	4.44[c]	-2.13	-1.18
HAD2	-1.55	-2.69	4.21[c]	4.21[c]	-5.76	-6.90
HBD1	2.68	2.37	4.24[c]	4.24[c]	-1.56	-1.87
HBD2	1.17	1.07	3.95[c]	3.95[c]	-2.78	-2.88

[a]This work, [b]Fe^{3+} chemical shift minus WT(Fe^{2+}) chemical shift, [c]Ref. 16, WT(Fe^{2+}), BMRB ID 5406.

Deprotonated Propionate 7

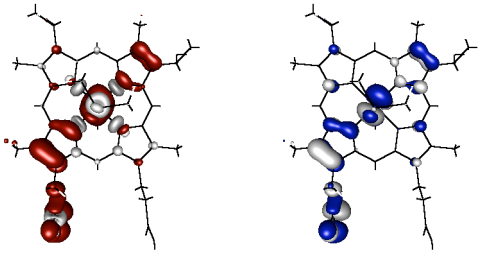

Spin Density Lowest-unoccupied, spin-down MO

Figure S1. PBE/TZVP DFT-computed unpaired spin density and lowest-unoccupied, spin-down molecular orbital (MO) for the model of heme *c* with a deprotonated propionate 7 side-chain. The similarity of the unpaired spin density and the lowest-unoccupied, spin-down MO of this model indicates that spin polarization is minimal.

Protonated Propionate 7

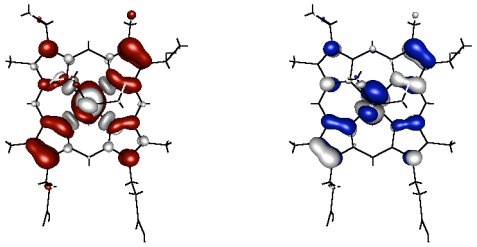

Spin Density Lowest-unoccupied, spin-down MO

Figure S2. PBE/TZVP DFT-computed unpaired spin density and lowest-unoccupied, spin-down molecular orbital (MO) for the model of heme *c* with a protonated propionate 7 side-chain. The similarity of the unpaired spin density and the lowest-unoccupied, spin-down MO of this model indicates that spin polarization is minimal.

Complete Citation for Reference 1

1. Morison, I. M.; Cramer Bordé, E. M.; Cheesman, E. J.; Cheong, P. L.; Holyoake, A. J.; Fichelson, S.; Weeks, R. J.; Lo, A.; Davies, S. M. K.; Wilbanks, S. M.; Fagerlund, R. D.; Ludgate, M. W.; Tatley, F.; Coker, M. S. A.; Bockett, N. A.; Hughes, G.; Pippig, D. A.; Smith, M. P.; Capron, C.; Ledgerwood, E. C. *Nature Genet.* **2008**, *40*, 387-389.

Cartesian Coordinates for all Computational Geometries Discussed in this Work

Deprotonated Propionate 7 Model

Fe	0.000000	0.000000	0.000000
C	0.011024	-3.406015	0.223964
C	-3.423340	-0.003175	-0.147551
C	-0.013104	3.416319	0.067700
C	3.416294	0.000000	-0.219977
N	-1.409721	-1.406845	0.027686
C	-1.222377	-2.770393	0.153543
C	-2.495122	-3.463547	0.145304
C	-3.469531	-2.498409	0.004217
C	-2.781989	-1.228160	-0.056902
C	-4.950576	-2.680024	-0.071600
C	-2.676617	-4.948159	0.236847
C	-2.611799	-5.637256	-1.134832
C	-2.760761	-7.139560	-1.044303
O	-2.889214	-7.783857	-0.018509
O	-2.730965	-7.712848	-2.278224
N	-1.429148	1.422112	-0.022303
C	-2.794234	1.234719	-0.113570
C	-3.497817	2.500911	-0.124826
C	-2.531853	3.478889	-0.017881
C	-1.249867	2.787779	0.025624
C	-4.980818	2.656195	-0.237965
C	-2.692376	4.966085	0.052404
C	-3.620311	5.453536	1.169985
N	1.417590	1.412644	-0.018631
C	1.222243	2.779500	0.026445
C	2.484335	3.483666	-0.045179
C	3.464457	2.513669	-0.155495
C	2.784354	1.236385	-0.142731
C	2.634791	4.971097	-0.015631
C	4.951856	2.690322	-0.259623
C	5.574641	3.484790	0.890904
N	1.420220	-1.413044	0.014943
C	2.784816	-1.228919	-0.127752
C	3.483304	-2.500525	-0.100762
C	2.521752	-3.467463	0.074456
C	1.244050	-2.774197	0.134413
C	4.962951	-2.667563	-0.227727
C	2.707658	-4.949703	0.190682
C	2.789362	-5.426375	1.648868
C	2.931804	-6.927254	1.767539
O	2.904922	-7.722124	0.844509
O	3.092783	-7.306646	3.064345
S	-3.340111	5.682813	-1.560664
S	5.311598	3.462427	-1.933582
C	-0.021478	0.659987	-4.150044
N	-0.023243	-0.716990	-4.082105
C	-0.009211	1.097981	-2.849108
C	-0.009541	-1.087083	-2.779602
N	-0.000000	0.000000	-2.007810
C	1.668288	0.084181	2.996758
S	-0.021457	-0.150422	2.346933
C	-0.847072	1.301089	3.090411
H	0.009011	-4.491784	0.317283
H	-4.510957	-0.013700	-0.212756
H	0.001665	4.504744	0.099386
H	4.500232	-0.011863	-0.327013
H	-5.472792	-2.089019	0.696458

H	-5.229295	-3.731980	0.071679
H	-5.347707	-2.362596	-1.048827
H	-3.646638	-5.173900	0.703607
H	-1.916715	-5.391296	0.897621
H	-3.396469	-5.255748	-1.807343
H	-1.657260	-5.423962	-1.642844
H	-5.233017	3.605742	-0.728246
H	-5.468177	2.647600	0.750504
H	-5.430322	1.846734	-0.829880
H	-1.713270	5.436559	0.201880
H	-3.639999	6.551882	1.200497
H	-3.250929	5.088452	2.138892
H	-4.648643	5.093023	1.039311
H	3.582698	5.280134	-0.472936
H	2.614399	5.355961	1.017265
H	1.823911	5.471050	-0.564042
H	5.427400	1.702797	-0.292342
H	5.203321	4.516177	0.928144
H	6.668269	3.517578	0.787406
H	5.337684	2.995364	1.848524
H	5.239012	-3.728571	-0.280820
H	5.495681	-2.231193	0.632261
H	5.351179	-2.175094	-1.132543
H	1.888052	-5.482699	-0.314475
H	3.626361	-5.250026	-0.334126
H	1.891069	-5.130707	2.215376
H	3.637108	-4.957039	2.172110
H	3.166775	-8.284647	3.071755
H	-2.366587	5.161086	-2.355291
H	6.666834	3.479170	-1.797089
H	-0.028343	1.194930	-5.092092
H	-0.032932	-1.354646	-4.873486
H	-0.005365	2.111873	-2.468185
H	-0.007457	-2.115208	-2.437612
H	1.622234	0.022728	4.090857
H	2.077655	1.048841	2.676382
H	2.280853	-0.734173	2.604629
H	-0.371089	2.231259	2.761202
H	-0.789736	1.196556	4.180835
H	-1.894397	1.278623	2.771588

Protonated Propionate 7 Model

Fe	0.000000	0.000000	0.000000
C	0.011024	-3.406015	0.223964
C	-3.423340	-0.003175	-0.147551
C	-0.013104	3.416319	0.067700
C	3.416294	0.000000	-0.219977
N	-1.409721	-1.406845	0.027686
C	-1.222377	-2.770393	0.153543
C	-2.495122	-3.463547	0.145304
C	-3.469531	-2.498409	0.004217
C	-2.781989	-1.228160	-0.056902
C	-4.950576	-2.680024	-0.071600
C	-2.676617	-4.948159	0.236847
C	-2.611799	-5.637256	-1.134832
C	-2.760761	-7.139560	-1.044303
O	-2.889214	-7.783857	-0.018509
O	-2.730965	-7.712848	-2.278224
N	-1.429148	1.422112	-0.022303
C	-2.794234	1.234719	-0.113570
C	-3.497817	2.500911	-0.124826

C	-2.531853	3.478889	-0.017881
C	-1.249867	2.787779	0.025624
C	-4.980818	2.656195	-0.237965
C	-2.692376	4.966085	0.052404
C	-3.620311	5.453536	1.169985
N	1.417590	1.412644	-0.018631
C	1.222243	2.779500	0.026445
C	2.484335	3.483666	-0.045179
C	3.464457	2.513669	-0.155495
C	2.784354	1.236385	-0.142731
C	2.634791	4.971097	-0.015631
C	4.951856	2.690322	-0.259623
C	5.574641	3.484790	0.890904
N	1.420220	-1.413044	0.014943
C	2.784816	-1.228919	-0.127752
C	3.483304	-2.500525	-0.100762
C	2.521752	-3.467463	0.074456
C	1.244050	-2.774197	0.134413
C	4.962951	-2.667563	-0.227727
C	2.707658	-4.949703	0.190682
C	2.789362	-5.426375	1.648868
C	2.931804	-6.927254	1.767539
O	2.904922	-7.722124	0.844509
O	3.092783	-7.306646	3.064345
S	-3.340111	5.682813	-1.560664
S	5.311598	3.462427	-1.933582
C	-0.021478	0.659987	-4.150044
N	-0.023243	-0.716990	-4.082105
C	-0.009211	1.097981	-2.849108
C	-0.009541	-1.087083	-2.779602
N	-0.000000	0.000000	-2.007810
C	1.668288	0.084181	2.996758
S	-0.021457	-0.150422	2.346933
C	-0.847072	1.301089	3.090411
H	0.009011	-4.491784	0.317283
H	-4.510957	-0.013700	-0.212756
H	0.001665	4.504744	0.099386
H	4.500232	-0.011863	-0.327013
H	-5.472792	-2.089019	0.696458
H	-5.229295	-3.731980	0.071679
H	-5.347707	-2.362596	-1.048827
H	-3.646638	-5.173900	0.703607
H	-1.916715	-5.391296	0.897621
H	-3.396469	-5.255748	-1.807343
H	-1.657260	-5.423962	-1.642844
H	-2.826496	-8.680454	-2.149044
H	-5.233017	3.605742	-0.728246
H	-5.468177	2.647600	0.750504
H	-5.430322	1.846734	-0.829880
H	-1.713270	5.436559	0.201880
H	-3.639999	6.551882	1.200497
H	-3.250929	5.088452	2.138892
H	-4.648643	5.093023	1.039311
H	3.582698	5.280134	-0.472936
H	2.614399	5.355961	1.017265
H	1.823911	5.471050	-0.564042
H	5.427400	1.702797	-0.292342
H	5.203321	4.516177	0.928144
H	6.668269	3.517578	0.787406
H	5.337684	2.995364	1.848524
H	5.239012	-3.728571	-0.280820

H	5.495681	-2.231193	0.632261
H	5.351179	-2.175094	-1.132543
H	1.888052	-5.482699	-0.314475
H	3.626361	-5.250026	-0.334126
H	1.891069	-5.130707	2.215376
H	3.637108	-4.957039	2.172110
H	3.166775	-8.284647	3.071755
H	-2.366587	5.161086	-2.355291
H	6.666834	3.479170	-1.797089
H	-0.028343	1.194930	-5.092092
H	-0.032932	-1.354646	-4.873486
H	-0.005365	2.111873	-2.468185
H	-0.007457	-2.115208	-2.437612
H	1.622234	0.022728	4.090857
H	2.077655	1.048841	2.676382
H	2.280853	-0.734173	2.604629
H	-0.371089	2.231259	2.761202
H	-0.789736	1.196556	4.180835
H	-1.894397	1.278623	2.771588